Railton, C. J., Koh, B. P., & Craddock, I. J. (2004). The treatment of thin wires in the FDTD method using a weighted residuals approach. IEEE Transactions on Antennas and Propagation, 52(11), 2941 - 2949. [issue 11]. 10.1109/TAP.2004.835126

The Treatment of Thin Wires in the FDTD Method Using a Weighted Residuals Approach

Chris J. Railton, Boon Ping Koh, and Ian J. Craddock

***Abstract*—In this contribution, the problem of accurately representing thin wires within the finite-difference time-domain (FDTD) mesh is addressed by means of a method based on the weighted residual (WR) interpretation of the FDTD algorithm. Results for wire dipoles and wire transmission lines, obtained using the proposed method, are presented and compared to those obtained using existing techniques. It is shown that the proposed method yields results which are more accurate and are less dependent on the choice of cell size than other approaches and, in addition, lends itself well to being extended for more complicated structures. Details of the calculation of the update equations are given.**

***Index Terms*—Dipole antennas, finite-difference time-domain (FDTD) methods, wire antennas.**

I. Introduction

TRADITIONALLY the finite-difference time-domain (FDTD) method has been described in terms either of the finite difference approximation to the differential form of Ampere's and Faraday's laws [1] or, alternatively, to the discrete approximation to the integral forms of these laws [2]. In uniform media, it has been shown that these two descriptions are equivalent and lead to exactly the same update equations. When the problem to be solved contains material boundaries, however, especially if these boundaries do not coincide with the Cartesian coordinate system, these two approximations may be different. The integral form, in general, yields the more accurate results.

A third description has been given, based on the interpretation of FDTD as an instance of the weighted residual (WR) method. In this description, each field point in the mesh is associated with a basis function and a weighting function, each of which has finite support in such a way that neighboring functions do not overlap. Details of this can be found in [3]–[5]. It has also been shown in [6], that if the set of basis functions is chosen to be the same as the set of weighting functions, i.e., Galerkin's method, a system which is analogous to a passive electrical circuit is obtained. From this it follows that algorithms based on this formulation yield a numerically stable solution, subject only to a Courant condition on the time step. Although the time step must be less than for standard FDTD, it has been found that using a time step 0.7 of this value will give stable results in almost all cases.

Manuscript received August 28, 2003; revised February 13, 2004.

The authors are with the Centre for Communications Research, University of Bristol, Bristol BS8 1UB, U.K. (e-mail: chris.railton@bristol.ac.uk).

Digital Object Identifier 10.1109/TAP.2004.835126

In this paper it will be shown how the standard FDTD formulation and the thin wire formalism introduced by Holland, [7] can be expressed in terms of the WR interpretation. Such a re-interpretation gives more insight into the method and also paves the way for extension and modification. Following this, an analysis method for thin wires based choosing appropriate basis and weighting functions in the WR interpretation will be described in detail and results presented for the test cases of a wire dipole and a wire transmission line. It will be demonstrated that the proposed method has similar or superior accuracy to existing techniques and gives more consistent results over a wide range of FDTD cell sizes.

II. WR Interpretation of Standard FDTD

The basic WR interpretation of FDTD is described in [4] and summarized here for completeness.

Consider one of the six update equations in FDTD

$$\frac{\partial E_x}{\partial t} = \frac{1}{\varepsilon}\left(\frac{\partial H_z}{\partial y} - \frac{\partial H_y}{\partial z}\right). \tag{1}$$

If each component is expanded in a set of basis functions, for example $\{\phi_i^{E_x}\}$, such that

$$E_x(x,y,z,t) = \sum_i E_{xi}(t)\phi_i^{E_x}(x,y,z) \tag{2}$$

where E_{xi} are the time dependent amplitudes, (1) can be written as

$$\sum_i \frac{\partial E_{xi}}{\partial t}\phi_i^{E_x} = \frac{1}{\varepsilon}\left(\sum_i H_{zi}\frac{\partial \phi_i^{Hz}}{\partial y} - H_{yi}\frac{\partial \phi_i^{H_y}}{\partial z}\right) \tag{3}$$

Taking the inner product of (3) with a set of test functions, $\{\psi_t^{E_x}\}$ yields

$$\sum_i \frac{\partial E_{xi}}{\partial t}\left\langle \psi_t^{E_x}, \phi_i^{E_x}\right\rangle = \frac{1}{\varepsilon}\left(\sum_i H_{zi}\left\langle \psi_t^{E_x}, \frac{\partial \phi_i^{H_z}}{\partial y}\right\rangle - H_{yi}\left\langle \psi_t^{E_x}, \frac{\partial \phi_i^{H_y}}{\partial z}\right\rangle\right). \tag{4}$$

If the basis and weighting functions are chosen such that

$$\left\langle \psi_i^{E_x}, \phi_i^{E_x}\right\rangle = C_i^{E_x}$$
$$\left\langle \psi_j^{E_x}, \phi_i^{E_x}\right\rangle = 0 \qquad i \neq j \tag{5}$$

where $C_i^{E_x}$ is a positive constant, the summation on the left hand side can be removed and a fully explicit update equation for E_x is obtained. This can be written concisely as follows:

$$\frac{\partial E_{xt}}{\partial t} = \frac{1}{\varepsilon C_t^{E_x}} \sum_i \left(H_{zi} g_{E_{xt}H_{zi}} - H_{yi} g_{E_{xt}H_{yi}} \right) \tag{6}$$

where

$$\begin{aligned} g_{E_{xt}H_{yi}} &= \left\langle \psi_t^{E_x}, \frac{\partial \phi_i^{H_y}}{\partial z} \right\rangle \\ g_{E_{xt}H_{zi}} &= \left\langle \psi_t^{E_x}, \frac{\partial \phi_i^{Hz}}{\partial y} \right\rangle. \end{aligned} \tag{7}$$

Each FDTD node has associated with it a value, C and each link between nodes is associated with a value, g. These values, which depend only on the choice of basis and weighting functions, are analogous to capacitors and gyrators in an equivalent passive electrical circuit [6]. The other five update equations are dealt with in a similar way.

If all basis and test functions are chosen to be pulse functions centred on the node with which they are associated and occupying a volume equal to that of the cell, the standard FDTD update equations are recovered. However, it is possible to use any basis and test functions and, so long as they have the same finite support as the original pulse functions, the explicit nature of the algorithm is preserved. When dealing with thin wires and other geometrical details, the accuracy of the algorithm can be considerably improved by choosing basis functions which conform to the asymptotic behavior of the fields in the vicinity.

III. Thin Wire Formalisms

Three distinct approaches to the problem of representing thin wires in the FDTD method have been identified as follows:

1) Introduced by Holland [7] in 1981 and later extended by Ledfelt [8], Edelvik [9], and Bérenger [10]. This approach involves the introduction of an extra differential equation which relates the charge and current on the wire to the surrounding electric field.
2) Introduced by Umashankar and Taflove *et al.* [11] in 1987, [2] in 1988, and later extended by Boonzaier [12] Douglas [13], Makinen [14], Bingle [15], and Nadobny [16] based on the contour integration interpretation which involves field integration over the edges and faces of the cells.
3) Introduced by Railton [3] in 1994 and extended by Craddock [4], in 1998 based on modifying the basis and weighting functions in the WR interpretation.

The second method does not lend itself to a description in terms of a WR interpretation. The first method, although originally formulated from quite different point of view, can benefit from a re-interpretation in terms of WR and such a reformulation will be presented in this paper. The third method is developed completely within the WR point of view and is described in detail in this contribution.

A. Method 1—Auxiliary Differential Equation

This method and its derivatives involve the solution of an extra differential equation which relates the current and charge on the wire to the surrounding tangential electric field. While these methods have been shown to give good results, the formulation lacks rigour, particularly in the definition of the so-called "in cell inductance." This algorithm can be expressed more rigorously as a WR formulation in the following way.

In [7], it has been shown under the assumption of static conditions and with the wire orientated in the z direction that

$$E_z(r) = \frac{\mu}{2\pi} \ln\left(\frac{r}{a}\right) \left(\frac{\partial I}{\partial t} + c^2 \frac{d\lambda}{dz} \right) \tag{8}$$

where r is the radial distance from the wire, a is the wire radius, I is the current on the wire, λ is the charge per unit length and c is the phase velocity. Expanding E_z in a set of basis functions, $\{\phi_i^{Ez}\}$ gives

$$\sum_i E_{zi} \phi_i^{Ez}(r) = \frac{\mu}{2\pi} \ln\left(\frac{r}{a}\right) \left(\frac{\partial I}{\partial t} + c^2 \frac{d\lambda}{dz} \right). \tag{9}$$

Taking the inner product of both sides with a weighting function $\psi^w(r)$, gives

$$\sum_i E_{zi} \left\langle \phi_i^{Ez}, \psi^w \right\rangle = \frac{\mu}{2\pi} \left\langle \ln\left(\frac{r}{a}\right), \psi^w \right\rangle \left(\frac{\partial I}{\partial t} + c^2 \frac{d\lambda}{dz} \right) \tag{10}$$

or equivalently

$$\frac{\partial I}{\partial t} = \frac{\sum_i E_{zi} \left\langle \phi_i^{Ez}, \psi^w \right\rangle}{\frac{\mu}{2\pi} \left\langle \ln\left(\frac{r}{a}\right), \psi^w \right\rangle} - c^2 \frac{d\lambda}{dz}. \tag{11}$$

Following a similar procedure, the update equation for E_z can be written as

$$\sum_i \frac{\partial E_{zi}}{\partial t} \phi_i^{Ez}(r) = \frac{1}{\varepsilon} \left((\nabla \times H)_z - I\phi^w \right) \tag{12}$$

where ϕ^w is the assumed current density distribution. Note that, whereas in reality, the current is concentrated at the position of the wire, in the formulation of [7] it is considered to be distributed throughout a cylinder surrounding the wire, the shape of which is defined by the choice of basis function, $\phi^w(r)$. Taking the inner product with the E_z weighting functions gives

$$\frac{\partial E_{zi}}{\partial t} \left\langle \phi_i^{Ez}, \psi_i^{Ez} \right\rangle = \frac{1}{\varepsilon} \left(\left\langle (\nabla \times H)_z, \psi_i^{Ez} \right\rangle - I \left\langle \phi^w, \psi_i^{Ez} \right\rangle \right). \tag{13}$$

These two update equations (11) and (13), can be expressed as

$$\frac{\partial I}{\partial t} = \frac{1}{C_w} \sum_i E_{zi} g_{wi} - c^2 \frac{d\lambda}{dz} \tag{14}$$

$$\frac{\partial E_{zi}}{\partial t} = \frac{1}{\varepsilon C_{Ezi}} \left(\left\langle (\nabla \times H)_z, \psi_i^{Ez} \right\rangle - I g_{wi} \right) \tag{15}$$

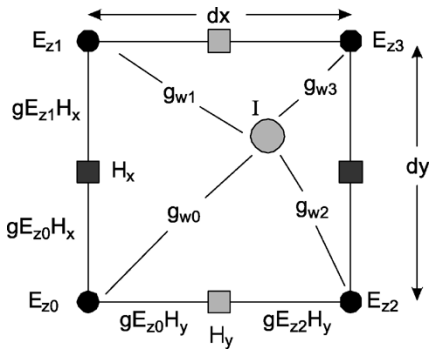

Fig. 1. Mesh for Holland's algorithm for a thin wire.

where, as before, each node has an associated equivalent circuit capacitor C, and each link between nodes has an associated equivalent circuit gyrator g. These are defined by

$$g_{wi} = \left\langle \phi^w, \psi_i^{Ez} \right\rangle \tag{16}$$

$$C_{Ezi} = \left\langle \phi_i^{Ez}, \psi_i^{Ez} \right\rangle \tag{17}$$

$$C_w = \frac{\mu}{2\pi} \left\langle \ln\left(\frac{r}{a}\right), \psi^w \right\rangle. \tag{18}$$

Referring to the equivalent circuit shown in Fig. 1, it can be seen that, in addition to the equivalent gyrators and capacitors which would be expected for the standard FDTD, there are four additional gyrators which link each current node on the wire with the four surrounding E_z nodes. Also, there is an equivalent capacitor associated with this I node.

Now, suppose all the basis and weighting functions are chosen to be pulse functions centred on their associated nodes and having finite support over a volume equal to the cell volume, but zero on the wire. In that case, update equations in agreement with those presented in [7] are obtained with the in-cell inductance being the same as $L_\square$ as given in equation (54) in [7]. For this choice of functions the following values for the equivalent circuit components are obtained, dx and dy are the lengths of the cell in the x and y direction, respectively, and β_x and β_y are the distances of the wire from the origin of the cell

$$g_{w0} = (dx - \beta_x)(dy - \beta_y) \tag{19}$$

$$g_{w1} = (dx - \beta_x)\beta_y \tag{20}$$

$$g_{w2} = \beta_x(dy - \beta_y) \tag{21}$$

$$g_{w3} = \beta_x \beta_y \tag{22}$$

$$C_{Ezi} = dxdy \tag{23}$$

$$C_w = \frac{\mu}{2\pi} \int_{-\frac{dy}{2}}^{\frac{dy}{2}} \int_{-\frac{dx}{2}}^{\frac{dx}{2}} \ln\left(\frac{r}{a}\right) dxdy. \tag{24}$$

Comparing (14) with [7, eq. (11)] shows that the in-cell inductance can be identified with C_{w} and $\langle E_z \rangle$ can be identified with $(1/dxdy)\sum_i E_{zi} g_{wi}$. Thus, using (24), the in-cell inductance can be written as

$$L = \frac{\mu}{2\pi dxdy} \int_{-\frac{dy}{2}}^{\frac{dy}{2}} \int_{-\frac{dx}{2}}^{\frac{dx}{2}} \ln\left(\frac{r}{a}\right) dxdy \tag{25}$$

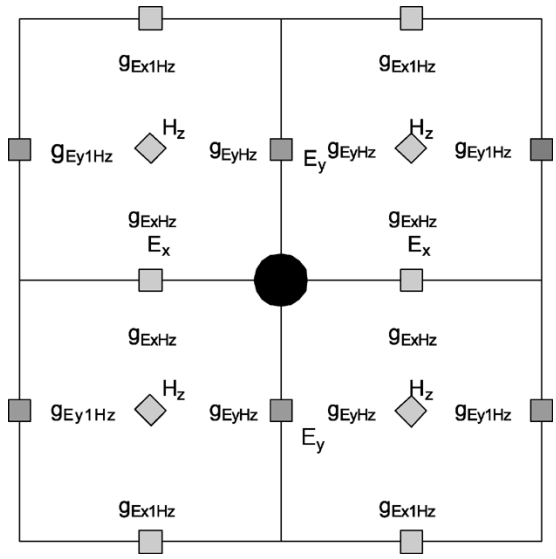

Fig. 2. Equivalent circuit components for a thin wire—TE plane ($z = 0$).

which is in agreement with [7, eq. (36)]. In that paper, it is shown that the integral can be performed analytically leading to [7, eq. (42)].

If the FDTD cells are square, i.e., $dx = dy$, and the current basis and weighting functions are chosen to be constant over a circular cylinder centred on the wire and having a radius of $dx/\sqrt{\pi}$, where dx is the cell size, then the equivalent circuit components become

$$g_{w0} = A_0 \tag{26}$$

$$g_{w1} = A_1 \tag{27}$$

$$g_{w2} = A_2 \tag{28}$$

$$g_{w3} = A_3 \tag{29}$$

$$C_{Ezi} = dxdy \tag{30}$$

$$C_w = \frac{\mu}{2\pi} \int_a^{\frac{dx}{\sqrt{\pi}}} \ln\left(\frac{r}{a}\right) dr \tag{31}$$

where, A_i is the area of the overlap between the circle, centred on the wire of radius $dx/\sqrt{\pi}$, and the rectangle centred on node E_{zi} and having the same dimensions as the cell. Making the same correspondence between [7, eq. (11)] and (14), it can be seen that the in-cell inductance is given as follows, in agreement with [7, eq. (12)]:

$$L = \frac{\mu}{dxdy} \int_a^{\frac{dx}{\sqrt{\pi}}} \ln\left(\frac{r}{a}\right) dr. \tag{32}$$

B. Method 2—Contour Integration Interpretation

The approach described in [11], and it's derivatives, derive modified update equations for some of the field components in the vicinity of the wire by consideration of the static field distribution near the wire. It can be shown that this approach is not amenable to a description in terms of the WR interpretation for the following reasons.

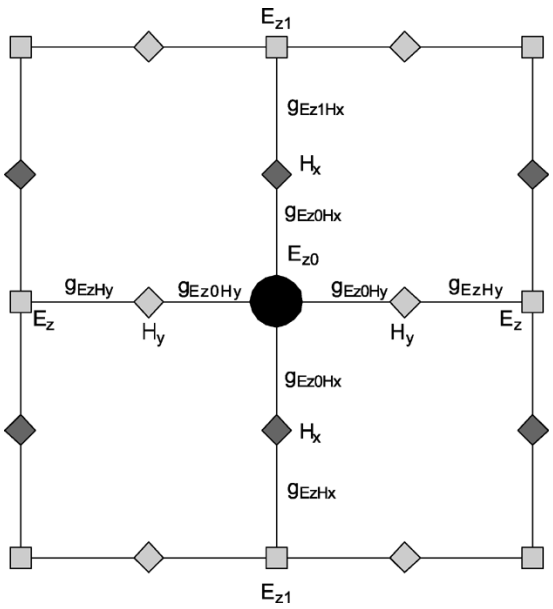

Fig. 3. Equivalent circuit components for a thin wire—TM plane ($z = dz/2$).

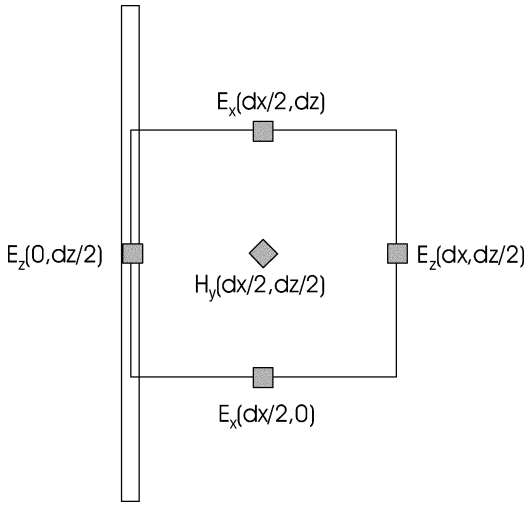

Fig. 4. Faraday's law contour path for thin-wire model.

In [11], the update equations for the H field nodes immediately next to the wire, and only these nodes, are modified. These are the H_x and H_y nodes shown in Figs. 2–4. Since the update equations of the E_z field nodes are not modified, the only way for this to conform to the WR description would be if the equivalent circuit capacitor associated with the H nodes, C_{Hx} and C_{Hy} was equal to $(1/2)\ln(dx/a)$ and $(1/2)\ln(dy/a)$, respectively, where a is the radius of the wire. Moreover, for consistency, C_{Ex}, C_{Ey}, and g_{ExHy} would also have to be set to this value. However, this would affect the update of the E_x and E_y nodes from the H_z nodes shown in Fig. 2. This is contrary to the method of [11]. In fact, there is no possible combination of equivalent circuit components which lead to the update equations given in [11].

C. Method 3—Modified Basis Functions

In this approach, as described in [4], the basis functions associated with the nodes in the vicinity of the wire are altered so they conform to the known asymptotic field behavior and boundary conditions. A Galerkin WR approach is then applied. Since the basis and test functions are zero on the wire, it is not necessary to explicitly calculate the current and no extra differential equations are involved.

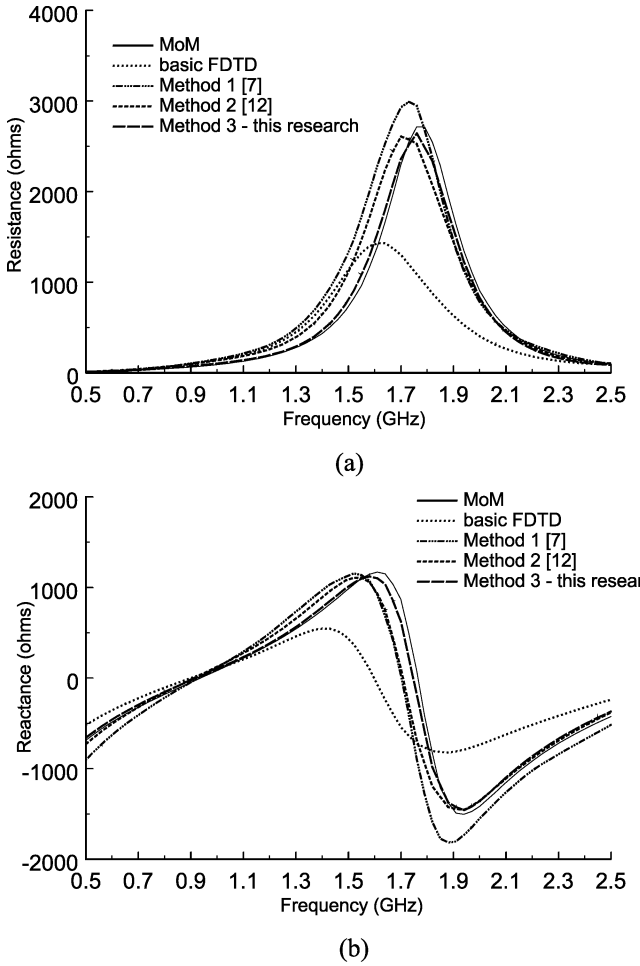

Fig. 5. Dipole radius 0.0625 mm: (a) terminal resistance and (b) terminal reactance. Cell size is 3 mm.

Consider the case where a thin wire of radius a, orientated in the z direction, which passes through the E_z nodes of the FDTD mesh. The asymptotic behavior of the fields are as follows:

$$E_z(r) \propto H_z(r) \propto \ln\left(\frac{\sqrt{x^2+y^2}}{a}\right) \tag{33}$$

$$E_x(x,y) \propto H_y(x,y) \propto \frac{x}{x^2+y^2} \tag{34}$$

$$E_y(x,y) \propto H_x(x,y) \propto \frac{y}{x^2+y^2}. \tag{35}$$

These functions, truncated to give the same support as the original pulse basis functions, can be used as basis functions for the nodes immediately adjacent to the wire. In this work, only uniform wires are treated and, therefore, cylindrical basis functions are used. The wire is considered to be terminated at an E_z node, i.e., on a TM plane as shown in Fig. 3. Future work will generalize this in order to take account of wire ends and corners.

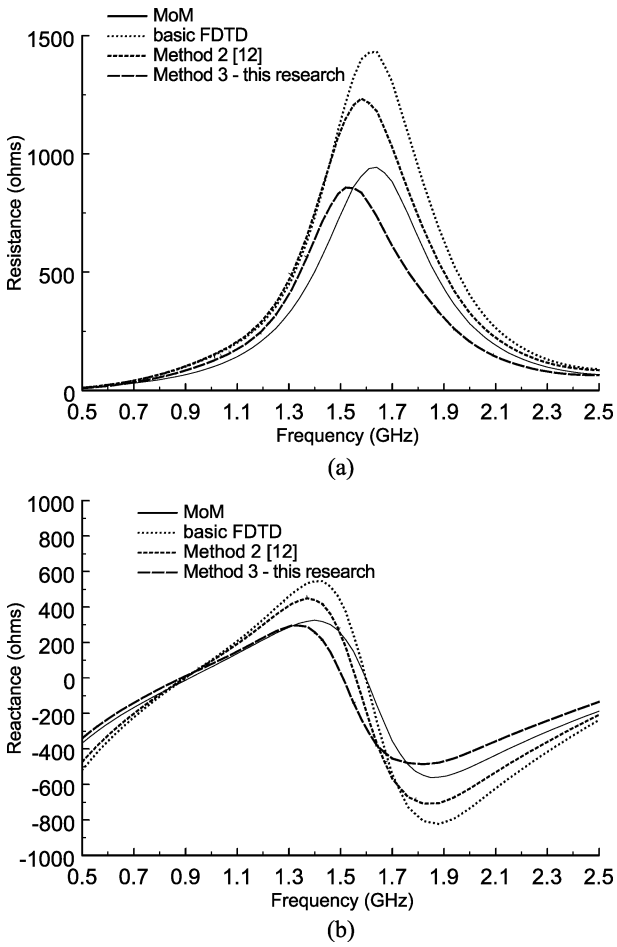

Fig. 6. Dipole radius 1 mm: (a) terminal resistance and (b) terminal reactance. Cell size is 3 mm.

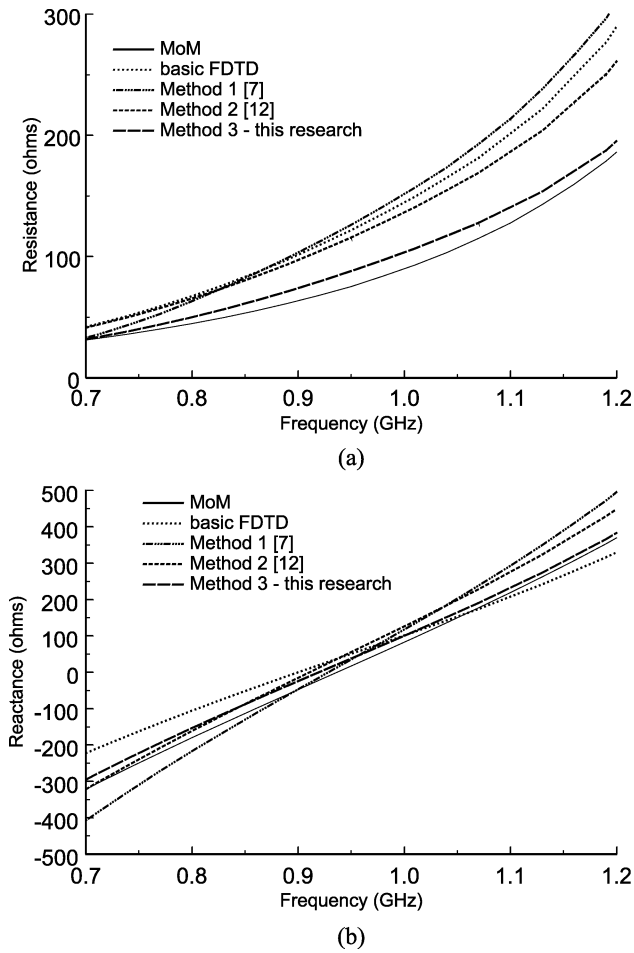

Fig. 7. Dipole radius 0.0625 mm: (a) terminal resistance and (b) terminal reactance. Cell size is 3 mm.

In [4], modified basis functions were used for the circumferential magnetic field components, leading to modified values for C_{Hy}, C_{Hx}, C_{Ey}, C_{Ex}, g_{EzHy} and g_{EzHx}. In this contribution, the asymptotic behavior of the other field components in the vicinity of the wire is also considered. This has resulted in improved accuracy, and the absence of nonphysical effects which were reported in [4].

IV. Update Equations for Method 3

In Fig. 2 and Fig. 3, the mesh immediately adjacent to a wire, shown by the large circle at the centres of the figures, is shown passing through the E_z nodes. The two planes are separated in the z direction by half the cell size. If all the neighboring nodes are to have their basis functions modified, it is necessary to calculate equivalent capacitors for nodes E_{z0}, E_y, H_y and H_z. In addition it is necessary to calculate the equivalent gyrators for the pairs of nodes $(E_{z0}H_y)$ (E_zH_y) (E_xH_z) $(E_{x1}H_z)$ $(E_{y1}H_z)$ and (E_xH_y). The remaining equivalent components are obtained from considerations of symmetry. Details of the required calculations are given in the Appendix. In terms of these values, the update equations for the affected nodes are as follows, where δx, δy, and δz are the cell sizes in the x, y, and z directions, respectively. δt is the time step and the node positions are relative to the position of the center of Fig. 2. It is noted that where the basis functions are unchanged from standard FDTD, the capacitor and gyrator values are unity. In this case they are not included in the update equations given below

$$\begin{aligned} &E_z^{n+1}\left(0,0,\frac{\delta z}{2}\right) \\ &\quad = E_z^n\left(0,0,\frac{\delta z}{2}\right)+\frac{\delta t}{\varepsilon C_{Ez0}} \\ &\qquad \times\left(g_{Ez0Hy}\left(H_y\left(\frac{\delta x}{2},0,\frac{\delta z}{2}\right)-H_y\left(-\frac{\delta x}{2},0,\frac{\delta z}{2}\right)\right)\right. \\ &\qquad \left.-g_{Ez0Hx}\left(H_x\left(0,\frac{\delta y}{2},\frac{\delta z}{2}\right)-H_x\left(0,-\frac{\delta y}{2},\frac{\delta z}{2}\right)\right)\right) \end{aligned} \quad (36)$$

$$\begin{aligned} &E_z^{n+1}\left(\delta x,0,\frac{\delta z}{2}\right) \\ &\quad = E_z^n\left(\delta x,0,\frac{\delta z}{2}\right)+\frac{\delta t}{\varepsilon\delta x\delta y\delta z} \\ &\qquad \times\left(\delta z\delta y H_y\left(\frac{3\delta x}{2},0,\frac{\delta z}{2}\right)-g_{EzHy}H_y\left(\frac{\delta x}{2},0,\frac{\delta z}{2}\right)\right. \\ &\qquad \left.-\delta x\delta z\left(H_x\left(\delta x,\frac{\delta y}{2},\frac{\delta z}{2}\right)-H_x\left(\delta x,-\frac{\delta y}{2},\frac{\delta z}{2}\right)\right)\right) \end{aligned} \quad (37)$$

$$E_z^{n+1}\left(0,\delta y,\frac{\delta z}{2}\right) = E_z^n\left(0,\delta y,\frac{\delta z}{2}\right)+\frac{\delta t}{\varepsilon\delta x\delta y\delta z} \times\left(\delta z\delta y\left(H_y\left(\frac{\delta x}{2},\delta y,\frac{\delta z}{2}\right)-H_y\left(-\frac{\delta x}{2},\delta y,\frac{\delta z}{2}\right)\right) -\delta x\delta z H_x\left(0,\frac{3\delta y}{2},\frac{\delta z}{2}\right)+g_{EzHx}H_x\left(0,\frac{\delta y}{2},\frac{\delta z}{2}\right)\right) \quad (38)$$

$$E_x^{n+1}\left(\frac{\delta x}{2},0,0\right) = E_x^n\left(\frac{\delta x}{2},0,0\right)+\frac{\delta t}{\varepsilon C_{Ex}} \times\left(g_{ExHz}\left(H_z\left(\frac{\delta x}{2},\frac{\delta y}{2},0\right)-H_z\left(\frac{\delta x}{2},-\frac{\delta y}{2},0\right)\right) -g_{ExHy}\left(H_y\left(\frac{\delta x}{2},0,\frac{\delta z}{2}\right)-H_y\left(\frac{\delta x}{2},0,-\frac{\delta z}{2}\right)\right)\right) \quad (39)$$

$$E_x^{n+1}\left(\frac{\delta x}{2},\delta y,0\right) = E_x^n\left(\frac{\delta x}{2},\delta y,0\right)+\frac{\delta t}{\varepsilon\delta x\delta y\delta z} \times\left(\delta x\delta z H_z\left(\frac{\delta x}{2},\frac{3\delta y}{2},0\right)-g_{Ex1Hz}H_z\left(\frac{\delta x}{2},\frac{\delta y}{2},0\right) -\delta x\delta y\left(H_y\left(\frac{\delta x}{2},\delta y,\frac{\delta z}{2}\right)-H_y\left(\frac{\delta x}{2},\delta y,-\frac{\delta z}{2}\right)\right)\right) \quad (40)$$

$$H_z^{n+\frac{1}{2}}\left(\frac{\delta x}{2},\frac{\delta y}{2},0\right) = H_z^{n-\frac{1}{2}}\left(\frac{\delta x}{2},\frac{\delta y}{2},0\right)+\frac{\delta t}{\mu C_{Hz}} \times\left(g_{Ex1Hz}E_x\left(\frac{\delta x}{2},\delta y,0\right)-g_{ExHz}E_x\left(\frac{\delta x}{2},0,0\right) -g_{Ey1Hz}E_y\left(\delta x,\frac{\delta y}{2},0\right)+g_{EyHz}E_y\left(0,\frac{\delta y}{2},0\right)\right) \quad (41)$$

$$H_y^{n+\frac{1}{2}}\left(\frac{\delta x}{2},0,\frac{\delta z}{2}\right) = H_y^{n-\frac{1}{2}}\left(\frac{\delta x}{2},0,\frac{\delta z}{2}\right)+\frac{\delta t}{\mu C_{Hy}} \times\left(g_{EzHy}E_z\left(\delta x,0,\frac{\delta z}{2}\right)-g_{Ez0Hy}E_z\left(0,0,\frac{\delta z}{2}\right) -g_{ExHy}\left(E_x\left(\frac{\delta x}{2},0,\delta z\right)-E_x\left(\frac{\delta x}{2},0,0\right)\right)\right) \quad (42)$$

$$H_x^{n+\frac{1}{2}}\left(0,\frac{\delta y}{2},\frac{\delta z}{2}\right) = H_x^{n-\frac{1}{2}}\left(0,\frac{\delta y}{2},\frac{\delta z}{2}\right)+\frac{\delta t}{\mu CHx} \times\left(gEyHx\left(E_y\left(0,\frac{\delta y}{2},\frac{\delta z}{2}\right)-E_y\left(0,\frac{\delta y}{2},-\frac{\delta z}{2}\right)\right) -g_{Ez1Hx}E_z\left(0,\delta y,\frac{\delta z}{2}\right)+g_{Ez0Hx}E_z\left(0,0,\frac{\delta z}{2}\right)\right) \quad (43)$$

The equations for the remaining nodes follow immediately from symmetry. It would also be possible to use modified basis functions for the nodes further from the wire but this has been found both unnecessary and also problematic when other objects are in the vicinity.

V. Results for a Wire Dipole

As an example of the application of this approach, results for the terminal impedance of two different dipoles are calculated. The first dipole has a length of 0.1545 m and a radius of 0.0625 mm, the second dipole has the same length but a radius of 1 mm. In each case, results are calculated using three different meshes. These have cell sizes of 3, 6, and 12 mm, respectively in the transverse directions and cell sizes of 2.575, 5.15, and 5.15 mm, respectively in the axial direction. A delta gap excitation source of unity voltage was used and the terminal impedance was calculated by probing the circumferential H field around the source and using Ampere's law to calculate the current.

Calculations were performed using standard FDTD, method 1 as described in [7], method 2 as described in [12], and method 3 as presented in this contribution. It was found that the results from [11] were indistinguishable from those obtained using the method of [12] so only the latter are included in the figures.

For comparison, results calculated using a MoM code are also plotted. This is an in-house code which uses piecewise sinusoidal basis and weighting functions and a delta gap source [17]. Five basis functions were used to model the dipole although it was found that this choice was not critical.

Results for a transverse cell size of 3 mm are shown in Figs. 5 and 6 for the two wire radii respectively, where it can be seen that method 3 gives results which are somewhat closer to those of the MoM reference than those obtained using methods 1 and 2. It can also be seen that the basic FDTD gives results which are not accurate, especially for very thin wires. Fig. 7 gives an enlarged view of the behavior of the predicted results at frequencies near the first resonance of the dipole. Again, it can be seen that the results from this research give better agreement to those obtained using the MoM code.

The values for the capacitors and gyrators used in these examples are given in Table I. It is noted that, in this case, g_{Ez0Hy} is zero and therefore the value of C_{Ez0} has no effect.

In Figs. 8–11, the results obtained using transverse cell sizes of 3, 6, and 12 mm are plotted for the case of methods 1, 2, and 3 and the basic FDTD method respectively. In each case results for a wire radius of 0.0625 and 1 mm are given. From Fig. 10 it can be seen that the results using Method 3 do not vary very much even if the cell size is changed by a factor of four. The results using methods 1 and 2, while also giving good consistency, do show more variation, especially for the thicker wire and the finer mesh where the wire has a radius of 1/3 the cell size. Finally, as would be expected, basic FDTD gives results which vary enormously with the cell size and are independent of the wire radius.

VI. Results for a Two Wire Transmission Line

As a second example of the use of the thin wire algorithms, the case of a transmission line formed by a wire over a ground plane is considered. This is formally the same as a twin wire

TABLE I
EQUIVALENT CAPACITOR AND GYRATOR VALUES FOR THE TEST DIPOLES

	Radius 0.0625mm			Radius 1mm		
	3mm	6mm	12mm	3mm	6mm	12mm
C_{Ez0}	8.32	12.7	17.8	0.10	0.80	2.25
C_{Ex}	1.49	1.76	2.02	0.40	0.67	0.93
C_{Ey}	1.49	1.76	2.02	0.40	0.67	0.93
C_{Hz}	1.01	1.00	1.00	1.31	1.09	1.04
g_{Ez0Hy}	0	0	0	0	0	0
g_{EzHy}	0.79	0.79	0.79	0.79	0.79	0.79
g_{ExHz}	1.49	1.66	1.82	0.92	1.02	1.16
g_{ExHy}	1.49	1.76	2.02	0.40	0.67	0.93

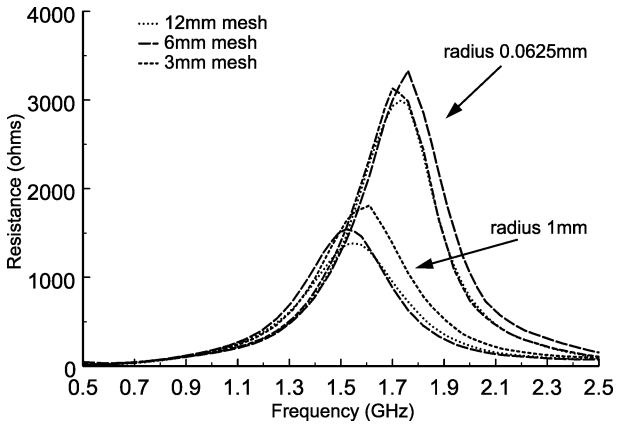

Fig. 8. Results for different mesh sizes—method 1 [6].

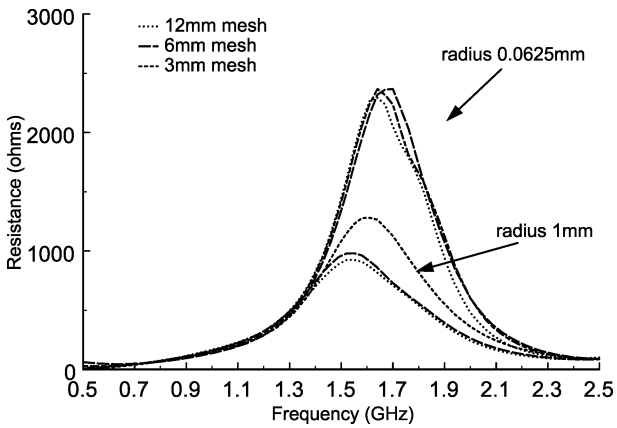

Fig. 9. Results for different mesh sizes—method 2 [12].

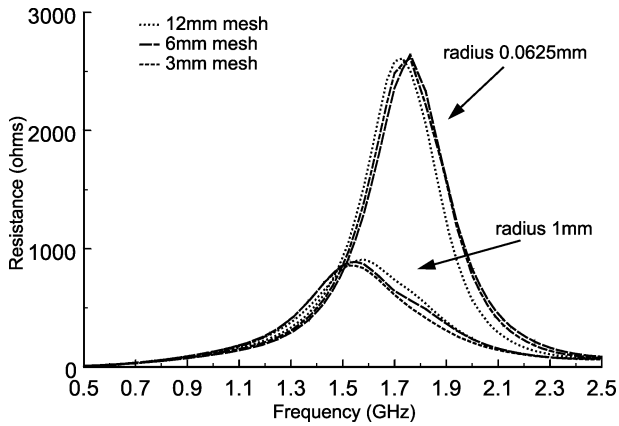

Fig. 10. Results for different mesh sizes—method 3 (this research).

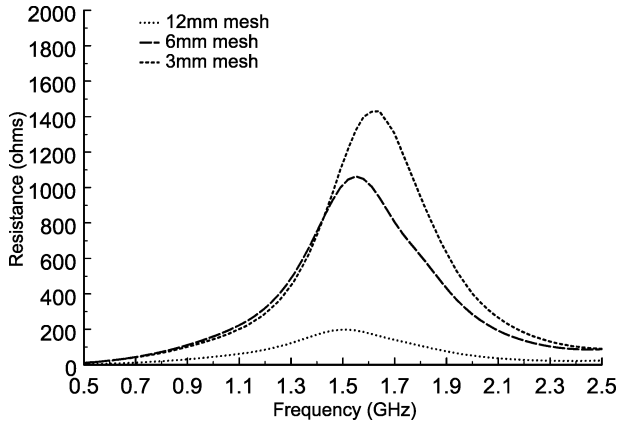

Fig. 11. Results for different mesh sizes—basic FDTD.

transmission line. This example, which appears less in the literature, has properties which make it susceptible to different types of approximation error than isolated dipoles or loops. In particular, the fields are much less symmetrical in this case and also, different parameters, such as characteristic impedance, are of interest.

Results for the characteristic impedance of a wire 10 mm above a ground plane and with radii varying from 0.05 to 0.5 mm are presented in Fig. 12. The mesh size used was 2 mm in all directions. These values were calculated by taking a snapshot of the fields in the cross-section of the transmission line and calculating the voltage and current on the line from the observed E and H fields.

It can be seen that method 2 [12], and an extended version of this method [14], give results which are, on average, much more accurate than those from basic FDTD, with the enhancement of [14] bringing the result closer to the analytical curve. The results obtained using method 3 are, however, in even better agreement with the analytical results.

The application of method 1 to this type of problem involves a number of issues which need to be considered. For instance there are several possible ways in which the voltage on the line can be obtained from the calculated field and charge density and this in turn leads to different predicted values for the characteristic impedance. The use of auxiliary differential equation methods to transmission line problems is the subject of a separate contribution.

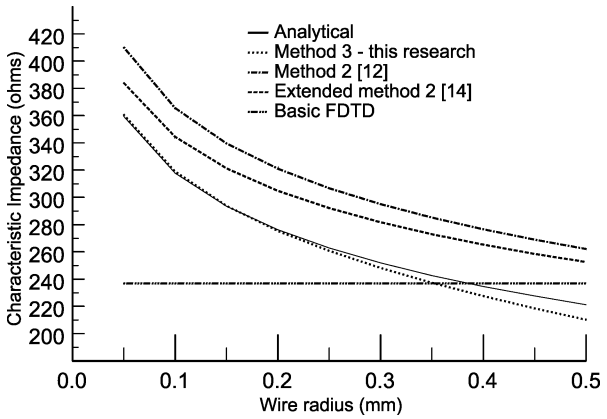

Fig. 12. Characteristic impedance of a two wire transmission line.

VII. Conclusion

In this contribution the use of the WR interpretation of FDTD for the solution of problems involving thin wires has been examined. Some existing methods have been reformulated using this approach and the use of modified basis functions has been examined in detail. It has been shown that, with the correct choice of basis functions, accurate results can be obtained with a minimal modification to the basic FDTD mesh. It has been shown that this method can provide better accuracy than other treatments of singular fields. In addition, this approach allows the logical and systematic extension to more complicated structures.

Appendix
Calculation of the Update Equation Parameters

In [4, eqs. (21)–(25)], the general three-dimensional (3-D) formulae for the calculation of the equivalent circuit capacitors and gyrators are given in cylindrical coordinates. In this work only uniform wires are being addressed and, therefore, the axial variation of the basis functions is constant. Thus, the volume integrals given in [4] may be reduced to 2-D integrals over the surface transverse to the wire as follows.

The equivalent circuit capacitors are given by

$$C_{Ez0} = \int_{-\frac{dx}{2}}^{\frac{dx}{2}} \int_{-\frac{dy}{2}}^{\frac{dy}{2}} \ln\left(\frac{\sqrt{x^2+y^2}}{a}\right)^2 dydx = 4\int_{0}^{\frac{dx}{2}} \int_{0}^{\frac{dy}{2}} \ln\left(\frac{\sqrt{x^2+y^2}}{a}\right)^2 dydx. \tag{44}$$

This can be evaluated by changing variables and splitting the area of integration into two parts and using a cylindrical coordinate system with $r = \sqrt{x^2+y^2}$ and $\theta = \tan^{-1}(y/x)$

$$C_{Ez0} = 4\left(\int_{0}^{\tan^{-1}\left(\frac{dy}{dx}\right)} \int_{a}^{\frac{dx}{2\cos(\theta)}} \ln\left(\frac{r}{a}\right)^2 rdrd\theta + \int_{\tan^{-1}\left(\frac{dy}{dx}\right)}^{\frac{\pi}{2}} \int_{a}^{\frac{dy}{2\sin(\theta)}} \ln\left(\frac{r}{a}\right)^2 rdrd\theta\right). \tag{45}$$

This can be simplified by making use of the fact that

$$\int \ln\left(\frac{r}{a}\right)^2 rdr = \frac{r^2}{2}\left(\ln\left(\frac{r}{a}\right)^2 - \ln\left(\frac{r}{a}\right) + \frac{1}{2}\right). \tag{46}$$

In a similar manner, the other equivalent capacitors are given by

$$C_{Hz} = 2\left(\int_{0}^{\tan^{-1}\left(\frac{dy}{dx}\right)} \int_{a}^{\frac{dx}{\cos(\theta)}} \left(\ln\left(\frac{r}{a}\right)\right)^2 rdrd\theta\right) \tag{47}$$

$$C_{Hy} = 2\left(\int_{0}^{\tan^{-1}\left(\frac{dy}{2dx}\right)} \int_{a}^{\frac{dx}{\cos(\theta)}} \left(\frac{\cos(\theta)}{r}\right)^2 rdrd\theta + \int_{\tan^{-1}\left(\frac{dy}{2dx}\right)}^{\frac{\pi}{2}} \int_{a}^{\frac{dy}{2\sin(\theta)}} \left(\frac{\cos(\theta)}{r}\right)^2 rdrd\theta\right). \tag{48}$$

Here again the integral over r has a simple analytic form

$$\int \left(\frac{\cos(\theta)}{r}\right)^2 rdr = \cos^2(\theta)\ln(r). \tag{49}$$

The equivalent circuit gyrators are given as follows:

$$g_{EzHx} = 2\left(\int_{0}^{\tan^{-1}\left(\frac{dx}{2dy}\right)} \int_{\frac{dy}{2\cos(\theta)}}^{\frac{dy}{\cos(\theta)}} \left(\frac{\cos(\theta)}{r}\right)^2 rdrd\theta + \int_{\tan^{-1}\left(\frac{dx}{2dy}\right)}^{\tan^{-1}\left(\frac{dx}{dy}\right)} \int_{\frac{dy}{2\cos(\theta)}}^{\frac{dx}{2\sin(\theta)}} \left(\frac{\cos(\theta)}{r}\right)^2 rdrd\theta + \int_{0}^{\frac{dx}{2}} \frac{\frac{dy}{2}}{\left(\frac{dy}{2}\right)^2 + x^2} dx\right) \tag{50}$$

$$g_{EzHy} = 2\left(\int_{0}^{\tan^{-1}\left(\frac{dy}{2dx}\right)} \int_{\frac{dx}{2\cos(\theta)}}^{\frac{dx}{\cos(\theta)}} \left(\frac{\cos(\theta)}{r}\right)^2 rdrd\theta + \int_{\tan^{-1}\left(\frac{dy}{2dx}\right)}^{\tan^{-1}\left(\frac{dy}{dx}\right)} \int_{\frac{dx}{2\cos(\theta)}}^{\frac{dy}{2\sin(\theta)}} \left(\frac{\cos(\theta)}{r}\right)^2 rdrd\theta + \int_{0}^{\frac{dy}{2}} \frac{\frac{dx}{2}}{\left(\frac{dx}{2}\right)^2 + y^2} dy\right) \tag{51}$$

$$g_{Ez0Hy} = 2\left(\int_0^{\tan^{-1}\left(\frac{dy}{dx}\right)} \int_a^{\frac{dx}{2\cos(\theta)}} \left(\frac{\cos(\theta)}{r}\right)^2 r dr d\theta + \int_{\tan^{-1}\left(\frac{dy}{dx}\right)}^{\frac{\pi}{2}} \int_a^{\frac{dy}{2\sin(\theta)}} \left(\frac{\cos(\theta)}{r}\right)^2 r dr d\theta - \int_0^{\frac{dy}{2}} \frac{\ln\left(\frac{1}{a}\sqrt{\left(\frac{dx}{2}\right)^2 + y^2}\right)\frac{dx}{2}}{\left(\frac{dx}{2}\right)^2 + y^2} dy \right) \quad (52)$$

$$g_{ExHz} = \left(\int_0^{\tan^{-1}\left(\frac{dy}{2dx}\right)} \int_a^{\frac{dx}{\cos(\theta)}} \left(\frac{\cos(\theta)}{r}\right)^2 r dr d\theta + \int_{\tan^{-1}\left(\frac{dy}{2dx}\right)}^{\frac{\pi}{2}} \int_a^{\frac{dy}{2\sin(\theta)}} \left(\frac{\cos(\theta)}{r}\right)^2 r dr d\theta - \int_a^{dx} \frac{x}{a} \ln\left(\frac{x}{a}\right) dx \right) \quad (53)$$

$$g_{Ex1Hz} = \left(\int_{\tan^{-1}\left(\frac{dy}{2dx}\right)}^{\tan^{-1}\left(\frac{dy}{dx}\right)} \int_{\frac{dy}{2\sin(\theta)}}^{\frac{dx}{\cos(\theta)}} \left(\frac{\cos(\theta)}{r}\right)^2 r dr d\theta + \int_{\tan^{-1}\left(\frac{dy}{dx}\right)}^{\frac{\pi}{2}} \int_{\frac{dy}{2\sin(\theta)}}^{\frac{dy}{\sin(\theta)}} \left(\frac{\cos(\theta)}{r}\right)^2 r dr d\theta + \int_a^{dx} \ln\left(\frac{x}{a}\right) dx \right) \quad (54)$$

REFERENCES

[1] K. S. Yee, "Numerical solution of initial boundary value problems involving Maxwell's equations in isotropic media," *IEEE Trans. Antennas Propagat.*, vol. AP-14, pp. 302–307, 1966.

[2] K. Umashankar, A. Taflove, and B. Becker, "Calculation and experimental validation of induced currents on coupled wires in an arbitrary shaped cavity," *IEEE Trans. Antennas Propagat.*, vol. AP-35, pp. 1248–1257, 1987.

[3] C. J. Railton, "The simple rigorous and effective treatment of thin wires and slots in the FDTD method," in *Proc. European Microwave Conf.*, Cannes, 1994, pp. 1541–1546.

[4] I. J. Craddock and C. J. Railton, "A new technique for the stable incorporation of static field solutions in the FDTD method for the analysis of thin wires and narrow strips," *IEEE Trans. Microwave Theory Tech.*, vol. 46, pp. 1091–1096, Aug. 1998.

[5] C. J. Railton, B. P. Koh, and I. J. Craddock, "A sub-cellular algorithm for wire transmission lines in the FDTD method," in *Proc. IEEE Antennas Propagation Symp.*, Columbus, OH, June 2003, pp. 976–979.

[6] I. J. Craddock, C. J. Railton, and J. P. McGeehan, "Derivation and application of an equivalent passive circuit for the FDTD algorithm," *Microwave and Guided Wave Lett.*, vol. 6, pp. 40–43, Jan 1996.

[7] R. Holland and L. Simpson, "Finite-difference analysis of EMP coupling to thin struts and wires," *IEEE Trans. Electromagn. Compat.*, vol. 23, pp. 88–97, May 1981.

[8] G. Ledfelt, "Hybrid Time-domain methods and wire models for computational electromagnetics," Ph.D. dissertation, Royal Institute Technol., Stockholm, 2001.

[9] F. Edelvik, "A new technique for accurate and stable modeling of arbitrarily orientated thin wires in the FDTD method," *IEEE Trans. Electromagn. Compat.*, vol. 45, pp. 416–423, May 2003.

[10] J. Bérenger, "A multiwire formalism for the FDTD method," *IEEE Trans. Electromagn. Compat.*, vol. 42, pp. 257–264, Aug. 2000.

[11] K. R. Umashankar, A. Taflove, and B. Becker, "Calculation and experimental verification of induced currents on coupled wires in an arbitrarily shaped cavity," *IEEE Trans. Antennas Propagat.*, vol. 35, pp. 1248–1257, Nov. 1987.

[12] J. J. Boonzaieer, "The radiation and scattering by thin wires—a finite difference time domain approach," Ph.D. dissertation, Faculty of Engineering, Univ. Pretoria, Feb. 1994.

[13] M. Douglas, M. Okoniewski, and M. A. Stuchly, "Accurate modeling of thin wire antennas in the FDTD method," *Microwave Opt. Technol. Lett.*, vol. 21, no. 4, pp. 261–265, 1999.

[14] R. M. Makinen, J. S. Juntunen, and M. A. Kivikoski, "An improved thin-wire model for FDTD," *IEEE Trans. Microwave Theory Tech.*, vol. 50, pp. 1245–1255, May 2002.

[15] M. Bingle, D. B. Davidson, and J. H. Cloete, "Scattering and absorption by thin metal wires in rectangular waveguide—FDTD simulation and physical experiments," *IEEE Trans. Microwave Theory Tech.*, vol. 50, pp. 1621–1627, June 2002.

[16] J. Nadobny, R. Pontalti, D. Sullivan, W. Wlodarczyk, A. Vaccari, P. Deuflhard, and P. Wust, "A thin-rod approximation for the improved modeling of bare and insulated antennas using the FDTD method," *IEEE Trans. Antennas Propagat.*, vol. 51, pp. 1780–1796, Aug. 2003.

[17] G. A. Thiele, "Wire antennas," in *Computer Techniques for Electromagnetics*, R. Mittra, Ed. New York: Pergamon, 1973.

Chris J. Railton received the B.Sc. degree in physics with electronics from the University of London, London, U.K., in 1974 and the Ph.D. degree in electronic engineering from the University of Bath, Bath, U.K., in 1988.

During 1974 to 1984, he worked in the Scientific Civil Service on a number or research and development projects in the areas of communications, signal processing and EMC. Between 1984 and 1987, he worked at the University of Bath on the mathematical modeling of boxed microstrip circuits. He currently works in the Centre for Communications Research, University of Bristol, Bristol, U.K., where he leads the Computational Electromagnetics group which is engaged in the development of new algorithms for electromagnetic analysis and their application to the design of MMIs, planar and conformal antennas, microwave and RF heating systems, EMC, high-speed interconnects, and optical waveguide components.

Boon Ping Koh, photograph and biography not available at the time of publication.

Ian J. Craddock was born in the South West of England in 1972. He received the B.Eng. and Ph.D. degrees from the University of Bristol, Bristol, U.K., in 1992 and 1995, respectively.

Since then he has been lecturing undergraduate courses at the University of Bristol and pursuing research interests that include computational electromagnetics, antennas, ground-penetrating radar, and microwave imaging of breast tumors.